Original Articles

Repetitive Transcorneal Alternating Current Stimulation Reduces Brain Idling State After Long-term Vision Loss

E.G. Sergeeva [a],[*], M. Bola [a], S. Wagner [a], S. Lazik [a], N. Voigt [a], C. Mawrin [b], A.G. Gorkin [c], W.J. Waleszczyk [d], B.A. Sabel [a], P. Henrich-Noack [a]

[a] Otto-von-Guericke University of Magdeburg, Medical Faculty, Institute of Medical Psychology, Magdeburg, Germany
[b] Otto-von-Guericke University of Magdeburg, Medical Faculty, Institute of Neuropathology, Leipziger Str. 44, 39120 Magdeburg, Germany
[c] Institute of Psychology, Russian Academy of Science, Moscow, Russia
[d] Nencki Institute of Experimental Biology, Warsaw, Poland

ARTICLE INFO

ABSTRACT

Background: Deafferentation of visual system structures following brain or optic nerve injury leaves cortical areas deprived of visual input. Deprived cortical areas have a reduced sensory information processing and are characterized with localized enhanced or synchronized rhythms believed to represent an "idling state".
Objective/hypothesis: We hypothesized that cortical idling can be modified with transcorneal alternating current stimulation (tACS) known to modulate cortical oscillations and thus change the functional state of the deafferented areas.
Methods: tACS was applied in rat model of severe optic nerve crush using a protocol similar to our clinical studies (200 μA, 2–8 Hz) for 5 treatment days right after the lesion and at the chronic stage (3 months later). EEG and VEP were recorded over the visual cortices. In vivo confocal neuroimaging of the retina and histology of the optic nerves were performed.
Results: Morphological investigations showed massive retinal ganglion cells death and degeneration of the optic nerves after crush. Visual loss was associated with increased EEG spectral power and lower coherence, indicating an "idling state". Stimulation induced a significant decrease of EEG power towards normal values. These effects were especially pronounced in the chronic stage.
Conclusion: Our results suggest that alternating current injected via the eye is able to modulate visually deprived brain areas and thus reduce cortical idling.

Introduction

There is considerable evidence that non-invasive current stimulations can alter visual system function both in animals and humans [1–17]. Some studies used transcranial direct current stimulation (DCS) applied over visual areas to modulate spontaneous activity and cortical excitability which changes phosphene thresholds and visual perception [2–5]. Other studies found transorbital DCS [1] and alternating current stimulation) (ACS) have therapeutic efficacy of reducing visual deficits in patients with optic neuropathy [9–15,17,18].

While the underlying mechanisms of such visual improvements are yet fully understood, in clinical studies brain electrophysiology alterations were noticed after ACS treatment. Specifically, alpha-band power reductions in EEG of patients with vision loss were significantly counteracted in occipital sites of optic nerve patients treated with ACS [14,18]. It was hypothesized that the applied current forces neuronal networks to propagate synchronous firing which, in turn, may induce a "re-learned synchronization response" [13,15]. Due to increased synchronization the injured visual system may react more sensitively to the reduced input which then leads to functional improvements [13,15].

The recent finding that brain network functional connectivity in the EEG alpha-band is reduced in patients with vision loss, and increased after ACS stimulation [19] also argues in favor of re-synchronization as a possible mechanism of ACS action to improve visual perception in patients. To further clarify these issues, so that pre- and post-lesion comparisons of the EEG can be made, we used the well established and standardized preclinical model of the rat partial optic nerve crush (ONC) [20–23]. We hypothesized that such damage may permanently alter spontaneous brain activity in the region of primary deafferentation. Specifically, we wished to investigate whether *transorbital* ACS (here: *transcorneal* ACS; tACS) can alter EEG spectral power and coherence in the acute phase after severe optic nerve damage and in a chronic stage of visual deafferentation. Furthermore, we wish to determine whether these EEG changes are related to any functional improvement as measured with visual evoked potentials (VEP).

Prior animal experiments provided evidence of enhanced survival of axotomized retinal ganglion cells (RGCs) under transcorneal stimulation conditions [24–29], but it is unknown if this neuroprotection relates to any brain activity changes or functional benefits [28,29]. To this end in vivo confocal imaging of the retina was chosen to quantify the number of surviving RGCs and histological examinations of the optic nerves were done to quantify optic nerve damage.

Materials and methods

Animals and experimental design

Male Lister hooded rats (Crl:LIS; incoming at 8 weeks of age) were kept on a 12-h light − 12-h dark cycle at an ambient temperature of 24−26 °C and humidity of 65%, one rat per cage to prevent damage to the head stages. Food and water access was available *ad libitum*. Prior to the experiment all rats were handled for 2 days and randomly assigned to the following groups: (i) ONC surgery/tAC stimulation (ONC/tACS); $n = 15$), (ii) ONC surgery/Sham stimulation (ONC/Sham; $n = 12$) and (iii) sham surgery/sham stimulation (Sham/Sham; $n = 9$).

The experimental schedule is presented in Fig. 1.

Three weeks before ONC, stereotactic intracerebral injections of fluorescent dyes were made to label RGCs and recording electrodes were implanted. Rats were allowed to recover 1 week after surgery, at which point baseline recordings were conducted 2 weeks before ONC (baseline 1). In recording Session I (acute stage) EEG data were acquired directly after ONC and animals stimulated (treatment 1 − T1, tACS1) (details see chapter "EEG and VEP"). On the 4th (T2, tACS2), 7th (T3, tACS3), 11th (T4, tACS4) and 14th (T5, tACS5) day post-lesion animals were also stimulated and EEG recordings were made (corresponding to tACS in the acute stage). On day 18 after ONC (follow-up 1 − FU1) and 7 weeks after ONC (FU2) EEG data were collected without stimulating the animals.

Session II was performed three months after ONC ("chronic stage") with the same schedule as the first series and comprised: a baseline at 3 months after ONC (baseline 2); then recordings on the 3rd (treatment 1 − T1, tACS1), 7th (T2, tACS2), 10th (T3, tACS3), 14th (T4, tACS4), 17th (T5, tACS5) after baseline 2 (corresponding to tACS in the chronic stage), on 21st day (FU1) and at two months (FU2) after baseline 2.

For morphological analysis of retinal ganglion cells a baseline scan with in vivo confocal neuroimaging (ICON) was performed 10 days prior to ONC. Animals were studied again with ICON on day 14 post-ONC.

Narcosis for surgery, ICON measurements, EEG/VEP recording and tACS stimulation was induced with i.p. application of Ketamine (75 mg/kg) and Xylazine (10 mg/kg).
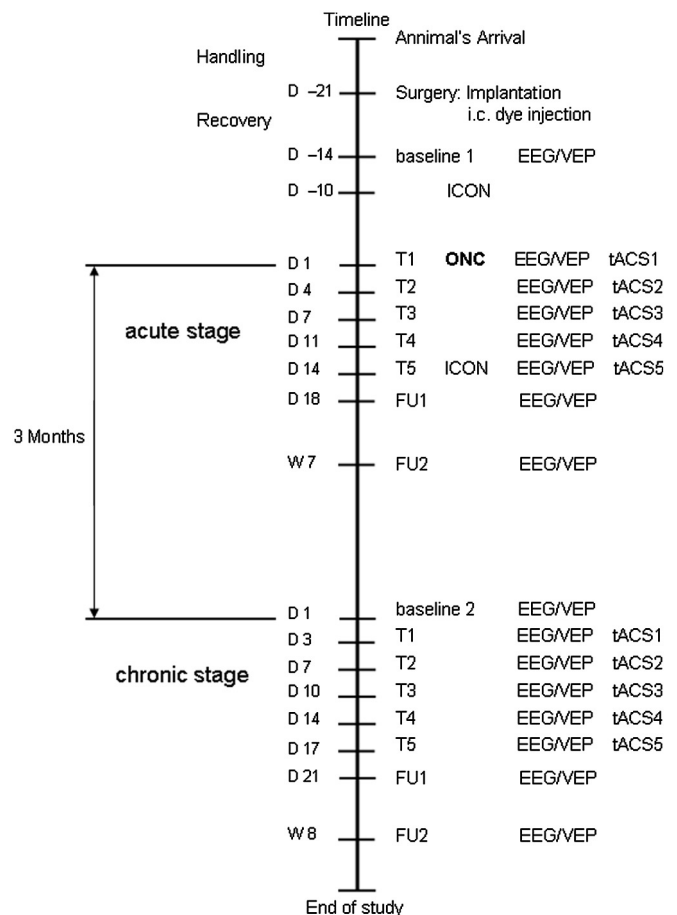

Figure 1. Experimental schedule. Numbers to the left of the time scale display the calendar time (D = day, W = week) and the numbers on the right represent the schedule of the procedures applied. The treatment immediately after ONC and on successive days corresponds to the "acute stage", and the treatment at three months after the ONC corresponds to the "chronic stage". For a detailed description see the text.

For all procedures ethical approval was obtained according to the requirements of the German National Act on the use of experimental animals.

Optic nerve crush

Both optic nerves were severely crushed using custom-made forceps as described in details by Sautter et al. [20,21]. Briefly, a lateral canthotomy was made and the optic nerve exposed by blunt dissection. The optic nerve crush was made with a calibrated forceps (Martin Instruments, Tuttlingen, Germany) applied for 30 s at a distance of 2−3 mm from the eye with the jaws of the forceps 0.1 mm apart. This narrow gap corresponds to a severe crush level ([20,21]). After surgery an antibiotic eye ointment (Aureomycin, Lederle Arzneimittel, Wolfratshausen, Germany) was applied. Sham operated animals underwent the same surgical procedure except that no optic nerve crush was applied.

In vivo confocal neuroimaging (ICON)

Labeling of RGCs

To label RGCs for in vivo imaging, stereotactic flourescent dye injections of 2 μl Oregon Green BAPTA; 10% in phosphate buffered saline with 0.1% DMS were made into both superior colliculi under

general anesthesia (as described above). To this end, the rat cranium was fixed in a stereotaxic head holder, and a hole was drilled in the skull at the bregma coordinates posterior − 6.9 mm, lateral 1.2 mm. The dye solution was then injected at each of the following depths below dura (0.5 µl injections each): 4.0 mm, 3.5 mm, 3.0 mm and 2.5 mm [28].

Data collection

ICON was carried out as described earlier [22,30].

Briefly, in anaesthetized rats the pupil was dilated (Neosynephrine-POS 2.5%; Ursapharm, Saarbrücken, Germany) and Vidisic optical gel was applied (M. Pharma, Berlin, Germany). The rats were then placed on a standard confocal scanning microscope (LSM 5 Pascal, Zeiss GmbH, Jena, Germany; 4× magnification) with the eye positioned underneath the objective lens. A −80 diopter lens (KPC-013, Newport GmbH, Darmstadt, Germany) was placed onto the cornea to adjust the focus point of the laser rays to the retina. Regions of interest for cell measurements were then determined according to Rousseau et al. [30]. All images were recorded with a 5× magnification objective lens. We used a scanning time of 24.5 s and an average of 16 scanning acquisitions. The procedure was carried out in both eyes at baseline and the eye with the best labeling was chosen for further investigations.

Images were taken from areas containing a sufficient number of cells which could be relocated at later time points using blood vessel morphology as landmarks. The number of fluorescent neurons at baseline (before ONC) was quantified and whether these cells still existed at the post-ONC data collection point was reassessed. On average we were able to evaluate the fate of 44 ± 12 neurons (mean ± SEM) per animal at baseline. This number was then set as 100% to have a common reference point for interindividual comparisons. For each animal the percentage of RGC survival could thus be calculated.

Statistical analysis

ICON data were analyzed with EXCEL and Graph Pad Prism software (GraphPad Software, Inc.). The outcome variables were described as means and the standard error of the means (SEM). Differences between groups were examined with t-tests for independent samples and were considered significant at $P \leq 0.05$ for two-tailed tests.

EEG and VEP

Surgery

Recording electrodes were implanted over the visual cortices as previously described by us [31]. Two stainless-steel screws with a shaft diameter of 1.17 mm (Fine Science Tools, Heidelberg, Germany) were stereotaxically inserted into the skull without piercing the dura. They were implanted bilaterally over the primary visual cortices 7 mm posterior to bregma and 3 mm lateral from midline to serve as EEG recording electrodes. A plastic ring was placed around the screws to prevent the skin from covering the assembly which was fixed with dental cement. Three stainless-steel surgical clamps were used as reference and neutral electrodes and were attached to the ears and the skin over the nose bone, respectively.

Data acquisition

Previously we have studied the dynamics of bioelectrical brain activity under Ketamine/Xylazine i.p. anesthesia in naive and lesioned animals and found that the depth of anesthesia influenced the tACS effects [31]. To prevent the known risk that deep narcosis counteracts any tACS effects we recorded EEGs only in the late stage of narcosis immediately before (PRE) and after (POST) tACS treatment.

Recording, reference and neutral electrodes were connected with wires to the EEG-device. During the transition stage of narcosis at about 35 min after administration the anesthetic agent (at which point delta activity declines and theta becomes dominant, see Ref. [31]), EEG recordings were started under normal room light conditions using electroencephalograph Encephalan-131-03, Modification 9 by Medicom MTD (Russia). The signal was acquired with a sampling rate of 256 Hz, bandwidth 0−100 Hz.

For VEP recordings a yellow LED source was placed 10 cm from rat's eye and 100 stimuli were delivered 1 per s (stimulus duration: 10 ms) before − pre and after − post EEG recording. The sequence of the recording sessions was as follows: pre VEP − pre EEG − tACS (or Sham) − pre EEG − pre VEP.

During the experiment the eyes of the rats were open and kept hydrated with Vidisic optical gel.

EEG and VEP analysis

Analysis of the EEG data was carried out in Matlab and EEGlab. Fragments (120 s) of the EEG signal recorded immediately before and after tACS were taken for analysis. We used offline linear finite impulse response filtering function (FIR) and applied a high-pass (0.5 Hz) FIR filter to exclude slow drifts, notch (50 Hz) FIR filter to exclude 50 Hz line, and low-pass (80 Hz) FIR filter to prevent aliasing during the following down-sampling to 250 Hz. Data were divided into non-overlapping 1 s long epochs.

Power density was calculated with the Matlab *pwelch* function, which divides each epoch into 8 sections (50% overlap), with each section Hamming windowed. The 8 periodograms were calculated and averaged. Power density was averaged over all epochs for each rat. Here power density was presented as normalized 10log10 values.

To investigate functional connectivity between visual cortices of two hemispheres we estimated coherence, indicating coupling between two signals as a function of frequency [32,33]. Using the Matlab function *mscohere* a coherence estimate was obtained for each data epoch and then matrices were averaged over epochs to give a coherence estimate for each recording, and over frequency bins, to give a coherence estimate for each EEG band.

In present study we focused on the whole spectrum and standard frequency ranges. Since we did not find significant differences between separate bands, here we show the results of integrated power and coherence in the range 0.5−80 Hz.

Visual evoked responses were averaged over 100 stimuli repetition. Minimum and maximum values within the time window of 0−150 ms were found for every averaged VEP trace and the peak-to-peak amplitude was calculated.

Data set structure and statistical analysis

Statistical analysis of EEG and VEP parameters was divided into four parts.

Firstly, to compare the three groups (ONC/tACS, ONC/sham, Sham/Sham) at baseline (before ONC) a one-way ANOVA was used with between-subjects factor "group" (3 levels: Sham/Sham, ONC/Sham, ONC/tACS).

Secondly, to elucidate immediate effects of the ONC (before the treatment) we used a repeated mixed linear model including between-subjects factor "group" (3 levels: Sham/Sham, ONC/Sham, ONC/tACS) and within subjects factor "lesion" (2 levels: before ONC, after ONC).

Thirdly, we investigated long-term effects of the treatment by comparing the recording after ONC (before treatment), FU1, and FU2 from two treatment sessions (acute and chronic). We used a mixed linear model including between-subjects factor "group" (3 levels: Sham/Sham, ONC/Sham, ONC/tACS), and within subjects factors "treatment session" (2: acute, chronic), "day" (3: baseline, FU1, FU2), and "time" (2: pre-, post-tACS).
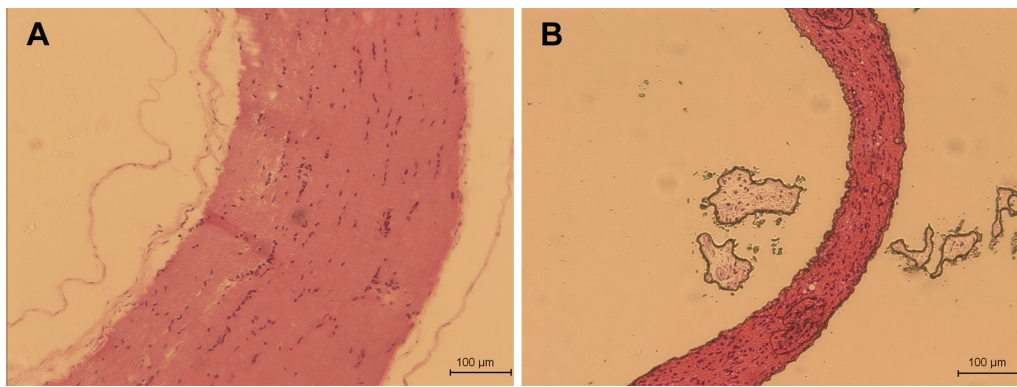
Figure 2. Histology of the optic nerves, photo 10× magnification. (A) Sham-lesioned animal. (B) Optic nerve 5 months after ONC.

Finally, to investigate EEG dynamics during the treatment, we analyzed data from five treatment days and from both the acute and chronic lesion sessions. Thus, the applied mixed linear model included between-subjects factor "group" (3 levels: Sham/Sham, ONC/Sham, ONC/tACS), and within subjects factors "treatment session" (2: acute, chronic),"day" (5: from treatment 1 to 5), and "time" (2: pre-, post-tACS).

Further, detailed comparisons between groups for each recording session were conducted with independent samples t-test. The Greenhouse–Geisser correction of multiple comparisons was applied. All statistical analyses were conducted with absolute values of EEG parameters. All statistical tests of significance used the $P < 0.05$ (two-tailed) as the criterion. All main effects and interactions were tested but only significant effects are mentioned in the text. Analysis was done in MatlabR2011b and SPSS 21 and displayed as mean ± standard error of the mean (SEM).

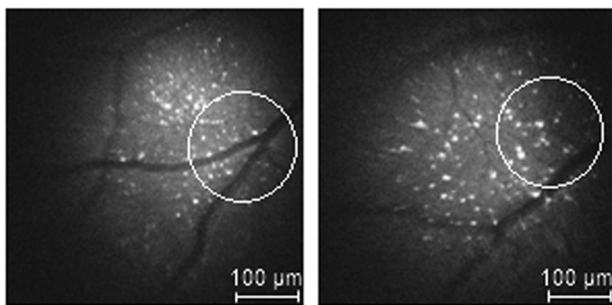*Transcorneal alternating current stimulation*

tACS treatment was given at different time points as outlined above (see Fig. 1). The stimuli consisted of biphasic square-wave pulses (pulse duration: 10 ms/phase, intensity: 200 μA) with changing frequencies. The stimulation protocol was based on clinical experience where a similarly modulated frequency schedule
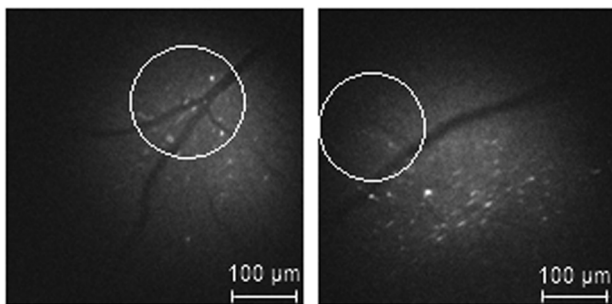

Figure 3. Neuronal loss in the retina after ONC (microphotographs of the same retinal area, relocated using blood vessel morphology as landmarks – white circled here). ICON data were collected at Baseline (top row) and on day 14 post crush (2nd row) for quantification of cell death. The crush leads to retinal ganglion cell degeneration with the majority of neurons being dead by day 14 (c.f. Rousseau et al., 2001; Prilloff et al., 2007; Leung et al., 2011).

Table 1
Statistical effects of studied factors and interactions.

Immediate ONC effects		
Spectral power		
Group × Lesion	$F(2,48) = 0.472$	$P = 0.627$
Coherence		
Group × Lesion	$F(2,51) = 0.594$	$P = 0.556$
VEP		
Group × Lesion	$\boldsymbol{F(2,43) = 4.66}$	$\boldsymbol{P = 0.015}$
Estimated effects for the treatment dynamics		
Spectral power		
Group	$\boldsymbol{F(2,356) = 35.74}$	$\boldsymbol{P < 0.001}$
Group × Session	$\boldsymbol{F(2,356) = 7.56}$	$\boldsymbol{P = 0.001}$
Session	$\boldsymbol{F(1,358) = 11.86}$	$\boldsymbol{P = 0.001}$
Time	$\boldsymbol{F(1,358) = 5.97}$	$\boldsymbol{P = 0.015}$
Day	$F(4,130) = 2.83$	$P = 0.27$
Coherence		
Group	$\boldsymbol{F(2,355) = 3.08}$	$\boldsymbol{P = 0.049}$
Group × Session	$\boldsymbol{F(2,355) = 4.30}$	$\boldsymbol{P = 0.015}$
Session	$\boldsymbol{F(1,359) = 53.09}$	$\boldsymbol{P < 0.001}$
Time	$\boldsymbol{F(1,359) = 34.41}$	$\boldsymbol{P < 0.001}$
Day	$F(4,143) = 2.85$	$P = 0.29$
VEP		
Group	$\boldsymbol{F(2,265) = 132.29}$	$\boldsymbol{P < 0.001}$
Group × Session	$\boldsymbol{F(2,265) = 24.51}$	$\boldsymbol{P < 0.001}$
Group × Time	$\boldsymbol{F(2,265) = 5.87}$	$\boldsymbol{P = 0.003}$
Session	$\boldsymbol{F(1,267) = 15.75}$	$\boldsymbol{P < 0.001}$
Time	$\boldsymbol{F(1,267) = 14.76}$	$\boldsymbol{P < 0.001}$
Estimated effects for the long-term changes		
Spectral power		
Group	$F(2,89) = 2.92$	$P = 0.059$
Day	$\boldsymbol{F(2,71) = 4.11}$	$\boldsymbol{P = 0.020}$
Coherence		
Group	$F(2,105) = 1.64$	$P = 0.198$
Group × Session	$\boldsymbol{F(2,105) = 3.88}$	$\boldsymbol{P = 0.023}$
VEP		
Group	$\boldsymbol{F(2,90) = 42.36}$	$\boldsymbol{P < 0.001}$
Group × Session	$\boldsymbol{F(2,90) = 7.38}$	$\boldsymbol{P = 0.001}$

Repeated mixed linear models include between-subjects factor "group" (3 levels: Sham/Sham, ONC/Sham, ONC/tACS) and within subjects factors "lesion" (2 levels: before ONC, after ONC), "treatment session" (2: acute, chronic), "day" (3: baseline, FU1, FU2) and "time" (2: pre-, post-tACS).
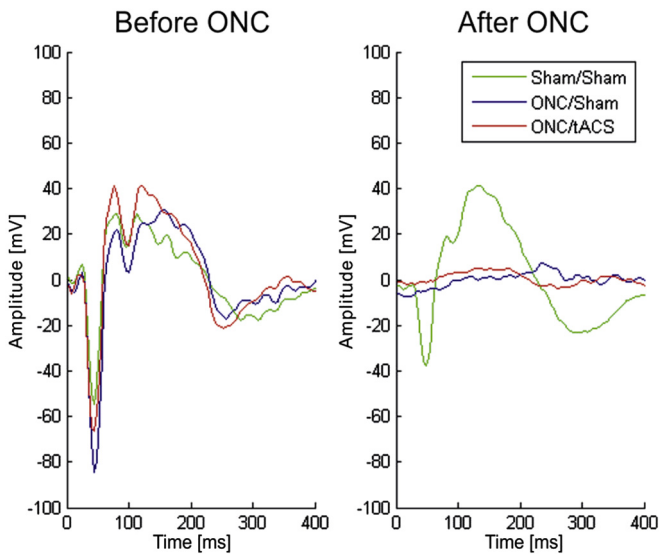Significant values are in bold type.

Figure 4. VEP averaged across groups before and after ONC. The shape of peaks and the amplitudes are similar on baseline recording while after ONC the evoked potentials disappeared in both lesioned groups.

was used in patients with optic nerve damage [14,18,19], but it was adjusted to rat's frequency dominating in a late stage of Ketamine/Xylazine narcosis [31] which is 5 Hz ± 3 Hz. Each tACS treatment session included two series with 120 s break between them. The series consisted of 35 cycles of bursts (15 pulses per burst, 420 pulses per cycle) of each frequency delivered alternating into one eye and another in the following order: 2-3-4-5-6-7-8-8-7-6-5-4-

3-2 Hz with 1 s break between bursts and 10 s break between cycles. Such stimulation session lasted about 23 min.

To carry out tACS, rats were first anaesthetized systemically with Ketamine/Xylazine and locally with Proparacain-POS 0.5%, and a 3 mm diameter gold ring electrode (Roland Consult, Brandenburg) was then placed on the rat's eyes after Vidisic optical gel had been applied to the cornea to protect it from drying and to assure best possible current conductance. The reference electrode was fixed on the tail. tACS was performed with a custom-made stimulator. Sham-treated animals underwent the same procedures except that no current was applied.

Histology of the optic nerve

At the end of the experiment animals were deeply anaesthetized (4 ml Chloral hydrate 8%; i.p.) and transcardially perfused with saline solution. Biopsy of the optic nerve was carefully performed, the tissue fixed by immersion and embedded in paraffin. One μm thick slices were cut on a microtome and the width of the axon was quantified after HE-staining with an Olympus BX60 microscope equipped with an Olympus DP50 camera. Software package Olympus cellD 3.1 was used to measure ON thickness.

Results

Histology of the optic nerve

Damage of the optic nerve after trauma was already visible during biopsy: whereas the nerves of the unlesioned rats were white/opaque, the nerves of the crushed animals were translucent. Measurements of the nerve width after HE-staining revealed that
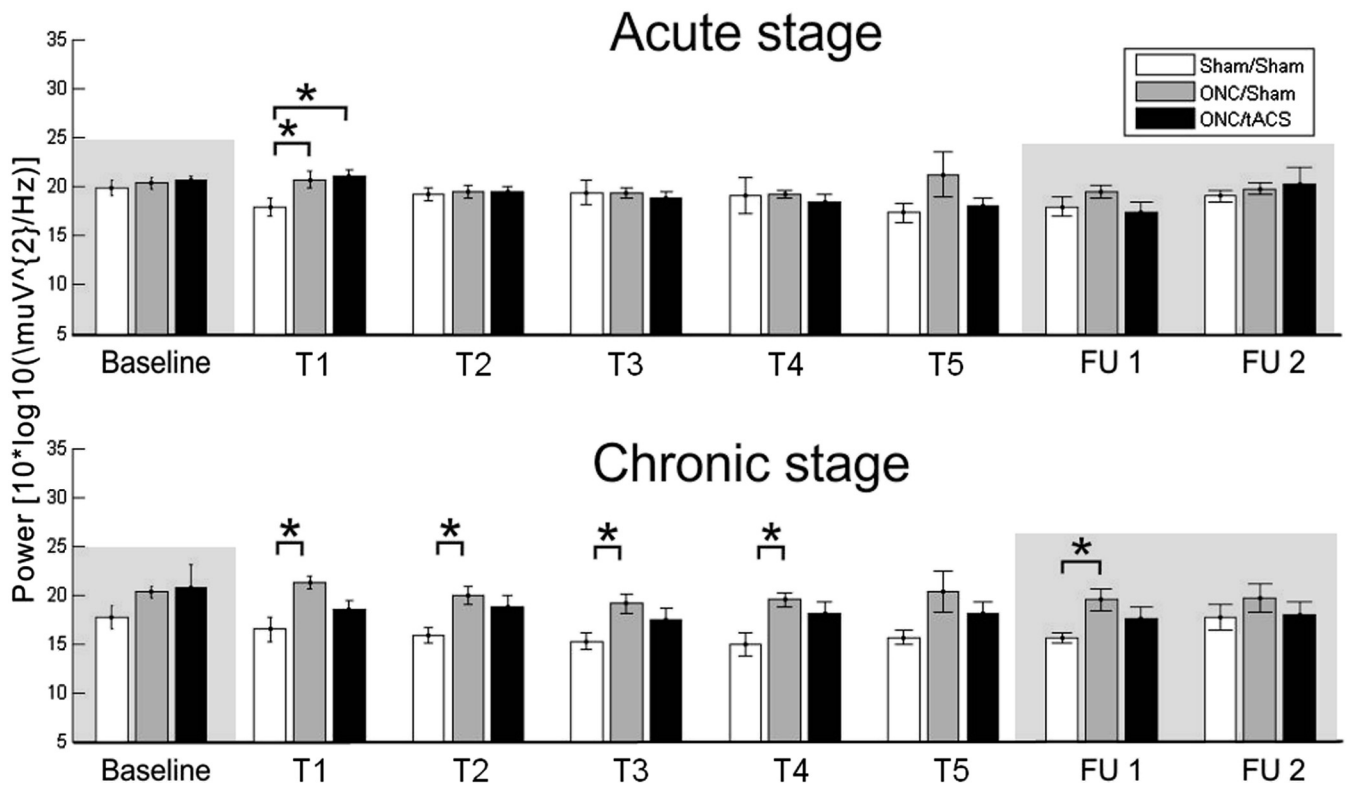

Figure 5. Spectral power of POST EEG (recorded after the stimulation) in three groups of rats in the acute and chronic stage. Results of two statistical models are presented: the bars with transparent gray background correspond to long-term effects of stimulation (baseline, FU1 and FU2). The bars without background correspond to the dynamics of treatment (T1-5). The spectral power in Sham/Sham (not lesioned and not stimulated) animals was significantly lower than in ONC/Sham (lesioned and not stimulated). And the power in ONC/tACS (lesioned and stimulated) was lower than in lesioned but not treated rats. *P < 0.05.

the crushed nerves were significantly thinner than the nerves of Sham/Sham rats (all data mean ± SEM; ONC/Sham: 225.9 ± 41.9 μm; ONC/tACS: 190.4 ± 34.8 μm; Sham/Sham: 360.0 ± 27.8 μm (one-way ANOVA $P = 0.02$; individual comparisons between groups (unpaired two-way Student's t-test) were as follows: Sham/Sham vs ONC/Sham; $P = 0.03$; Sham/Sham vs ONC/tACS: $P = 0.009$. The two groups which underwent ONC (ONC/tACS and ONC/Sham) were not statistically different ($P = 0.54$). Figure 2 shows a representative photomicrograph of an HE-stained lesioned and an unlesioned optic nerve.

ICON

Quantification of cell survival did not reveal a significant difference between sham- and tACS-treated rats 2 weeks after ONC which was statistically not different (percentage of survival (mean ± SEM): ONC/Sham $20.9 ± 14.3$ vs tACS $8.9 ± 4.6$; $P = 0.46$). In both groups a massive cell loss was detected which had been expected after the applying severe ONC conditions (Fig. 3) with an average of 15% RGCs survival.

Thus, morphological investigations confirmed the expected massive retinal ganglion cells death and the loss of their axons after ONC. There was no evidence of neuroprotective or regenerative influences of tACS on retinal neurons.

EEG and VEP

Baseline and immediate ONC effects

At baseline we did not find significant differences between groups for spectral power ($F(2,27) = 0.375$, $P = 0.691$), coherence ($F(2,27) = 1.025$, $P = 0.372$), and VEP ($F(2,25) = 0.78$, $P = 0.465$). ONC had no immediate effect on spectral power and coherence, but the amplitudes of VEP decreased significantly in ONC/Sham (t(1,6) = 6.18, $P < 0.001$) and ONC/tACS (t(1,10) = 5.31, $P < 0.001$), and no change in the control Sham/Sham group (t(1,6) = 0.951, $P = 0.373$) (Table 1; Fig. 4).

Treatment dynamics

We investigated treatment dynamics comparing data from five treatment days (T1-5) and two sessions. Long-term effects were evaluated by comparing before- and post-treatment data (Baseline vs. FU1 and FU2 in each session).

Spectral power. The statistical effects in ANOVA model are presented in the Table 1. Post-hoc comparisons showed significant differences between all three groups (all $P < 0.001$). The spectral power increased significantly immediately after ONC (T1 in Fig. 5), then treatment-by-treatment group differences during acute stage were not pronounced, though in mixed linear model, when averaged across treatment days (Fig. 6), both lesioned groups demonstrated increase power as compared to controls. This power increase in ONC rats was even greater at three months after lesion, and was significant on each day of recording. Most importantly, during the chronic stage the tACS-treated group showed a decreased EEG power approaching towards healthy control values.

The tendency towards an increased power as shown for treatment days was also present in long-term follow-up measurements: ONC/Sham group exhibited higher power than Sham/Sham group ($P = 0.052$). Interestingly, the decreased power in tACS-treated rats persisted up to FUs in the chronic stage (Fig. 5). Interestingly, we did not find any significant differences in spectral power between pre- and post-stimulation EEG (interaction between factor "group" and "time" in Table 1). This suggests the lack of an immediate after-effect following tACS.
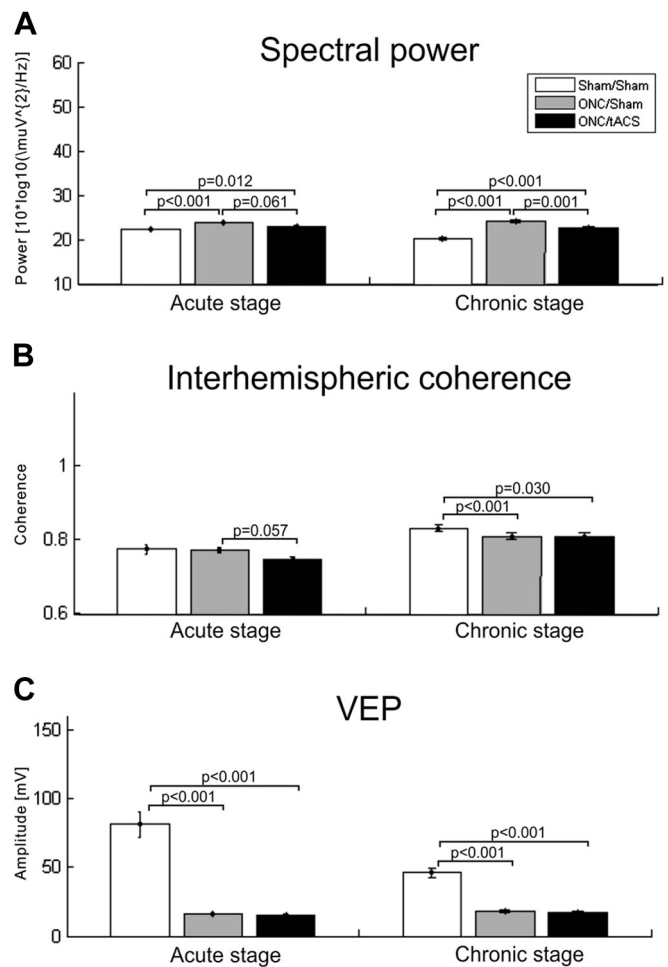

Figure 6. Profile plots showing the effect of factors group and session used in the mixed linear model describing treatment dynamics. (A) Spectral power of POST EEG averaged over the treatment days T1-5 in the acute stage and the chronic stage (three months after ONC). The power in lesioned animals was significantly higher than in non-lesioned controls, especially in the chronic stage. But the power in tACS-treated rats was lower than in non-treated, significantly only for the chronic stage. (B) Interhemispheric coherence of POST EEG averaged over the same time periods as in A. The coherence in lesioned animals was significantly lower on the chronic stage than in controls. (C) Peak-to-peak amplitude of POST VEPs averaged as above. The amplitude decreased after the ONC in lesioned animals with no signs of the VEP recovery.

Interhemispheric coherence. Though the factors in ANOVA model and their interactions showed the significant effects (Table 1), post-hoc tests revealed no difference between groups (all $P > 0.05$). The detailed comparisons of coherence did not detect considerable difference between groups on each day of stimulation and after the treatment on FUs (Fig. 7). But when averaged across treatment days in each session (acute and chronic) a significant drop of interhemispheric coherence in lesioned animals on chronic stage was observed (Fig. 6).

Visual evoked potentials. The main effects are shown in Table 1. A significant drop of VEP amplitudes was observed in both lesioned groups directly after ONC: Sham/Sham vs. ONC/tACS ($P < 0.001$), Sham/Sham vs. ONC/Sham ($P < 0.001$), and persisted over all experimental days without any recovery, neither spontaneously, nor due to tACS treatment: ONC/sham vs. ONC/tACS ($P = 0.592$) (Fig. 8). Profile plots for factors "group" and "session" are shown in Fig. 6. Like for treatment dynamics, we did not find any recovery of VEP on the FU days.
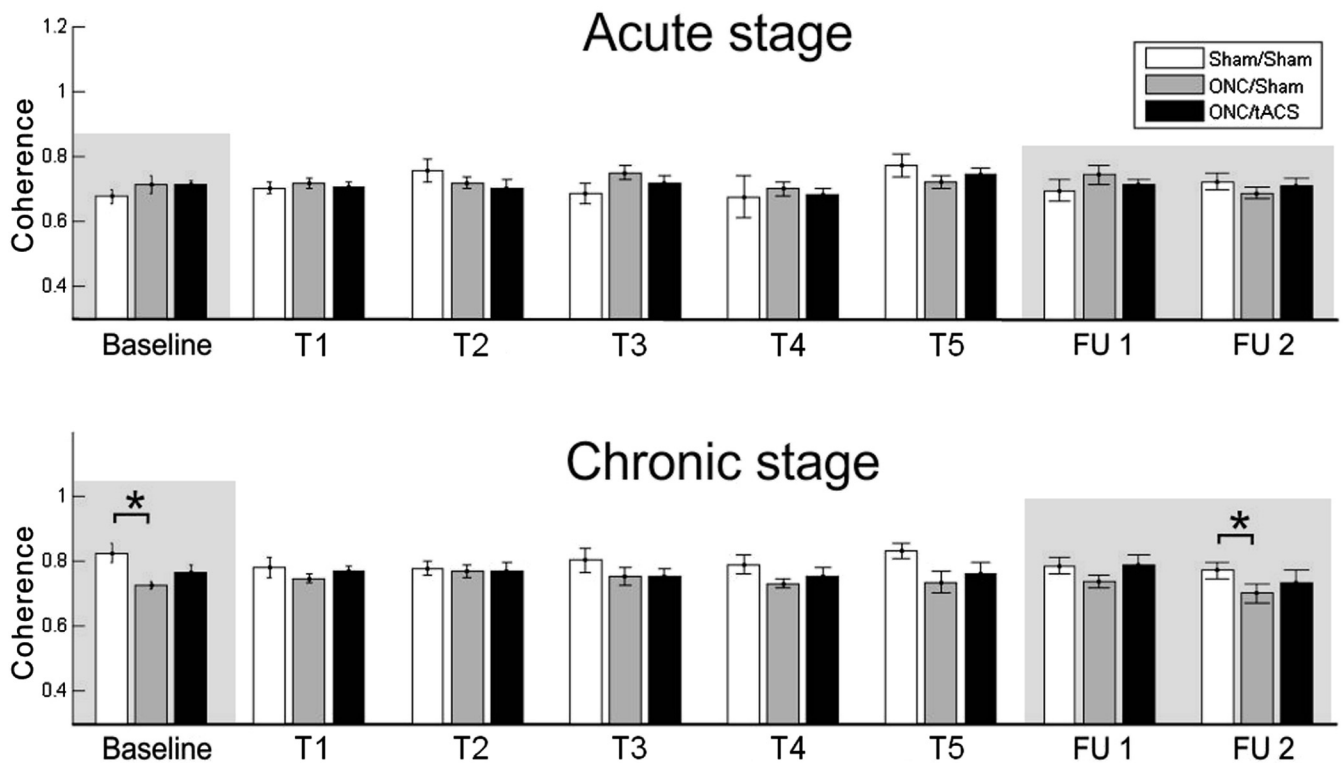
Figure 7. Interhemispheric coherence of POST EEG (recorded after the stimulation) in three groups in the acute and chronic stage. Results of two statistical models are presented: the bars with transparent gray background correspond to long-term effects of stimulation (baseline, FU1 and FU2). The bars without background correspond to the dynamics of treatment (T1-5). *$P < 0.05$.

Thus, the analysis of treatment dynamics and long-term effects showed that EEG power in animals with optic nerve crush was significantly higher than in non-lesioned controls, especially in the chronic stage. But the power in tACS-treated rats was lower than in non-treated ONC rats. The coherence in lesioned animals was significantly lower than in controls in the chronic stage. The amplitude of VEP decreased after ONC and did not recover, neither in non-treated nor in treated rats.

Discussion

Our model of severe optic nerve crush mimics the pathophysiology of partial but severe visual deafferentation. While a mild crush induces partially reversible damage [34], the more severe crush used here apparently leaves little chance for vision recovery and the rats remain functionally blind as shown with VEP (Fig. 4) or by behavioral brightness discrimination as shown before [28].

Electrophysiological consequences of the ONC

The loss of retinofugal activation after bilateral severe optic nerve lesion is so strong that little physiological drive reaches higher (cortical) visual areas and this may result in almost complete loss of input to the visual cortex. A similar situation has been described where bilateral visual deprivation was shown to induce degeneration of cells in the lateral geniculate body − which projects to visual cortex [35]. The lack of visual input following severe optic nerve damage reduces cortical information processing [36]. This visual deafferentation is expected to result in abnormal cortical function and dedifferentiation of individual experience which was shown long ago [37–43].

The concept of the idling state system

The situation when the visual cortex is neither receiving nor processing incoming visual information was described by Adrian and Matthews in 1934 [44] as an "idling system". Mulholland [45] differentiated "cortical work" from "cortical nil-work" for regions which are either processing or not processing sensory information at a specific point in time. It is this reduced "workload" in cortical areas which leads to a localized and enhanced (synchronized) rhythm. It is as if the brain's intrinsic oscillations, the "idling state", dominates the EEG when lack of sensory input fails to modulate this synchronization [45–51].

Interestingly, in a patient with chronic somatosensory deafferentation a significantly higher alpha-band spectral power was also observed in the resting state [52] which is in line with the hypothesis of a somatosensory "cortical idling" [53]. Also, the removal of tonic retinal inhibitory discharge through optic nerve damage [54,55] or a decrease in cortical inhibition after retinal lesion [56] can have an impact on the emerging idling of visual cortex.

In the present study we observed a significant increase in spectral EEG power in the chronic stage (as compared to normal controls) after severe optic nerve damage. We interpret this as an idling state of the visual cortex in rats that suffer long-term visual deafferentation.

tACS reduces idling after long-term visual loss

Since in ONC rats treated with tACS the EEG power was significantly lower than in non-treated ONC animals *we suggest that tACS is capable to alter the abnormal function of the deprived visual cortex and modulate it towards normal levels.* Note, however, that the EEG
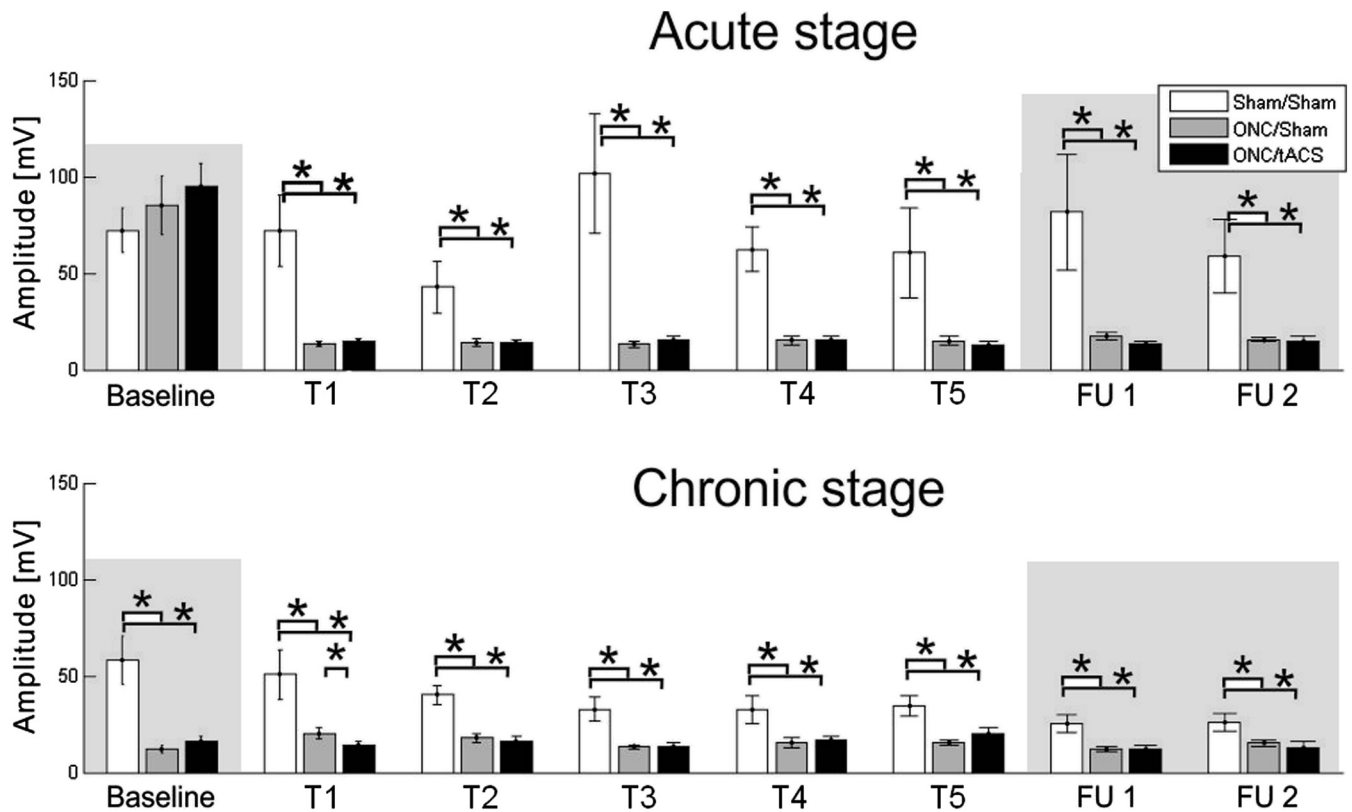
Figure 8. Peak-to-peak amplitude of POST VEP (recorded after the stimulation) in three groups in the acute and chronic stage. Results of two statistical models are presented: the bars with transparent gray background correspond to long-term effects of stimulation (baseline, FU1 and FU2). The bars without background correspond to the dynamics of treatment (T1-5).*$P < 0.05$.

power remained still above normal control values and this difference was most pronounced in the second tACS treatment block which was applied three months after the lesion.

One possible mechanism of the observed stimulation effect might be an excitation of the surviving (15%) RGCs which may induce potentials in visual cortex [57–61]; . It is conceivable that a minimum number of residual retinal cells and optic nerve axons is required and sufficient to induce such cortical changes. But given the strong lesion severity, the physiological activation of the retina and optic nerve by tACS is expected to be rather small. Moreover, in the present study we did not find any immediate after-effect of the stimulation (after each treatment). This argument is in line with our previous observations of aftereffects shown as a shift of theta power band towards higher frequencies following stimulation (with 8–13 Hz) which was seen only in healthy rats but not after severe optic nerve crush [31].

Another possible explanation could be based that there are non-functional cell networks in the brain (silent survivors) [28,29]. The current applied to the eye might be directed by the surviving axons inside the traumatized optic nerve. It is these remnants that might serve as a passive conductor of the current to enable the activation of distant brain structures, of which the LGN and the superior colliculus are of most interest for their connections with visual cortex. Further investigations are necessary to define whether such "silent survivors" may actually serve a useful purpose for rehabilitation treatments.

One may only speculate if the effects of tACS (decrease of spectral power), which is not visible after each stimulation and not pronounced in the acute stage, might cumulate across the treatment days and two sessions by day-to-day tACS-activation of the "gradually declining" system, and hence slow the progress of the deafferentation-induced idling.

Conclusion

In conclusion, we propose that the amount of residual structures is a factor influencing which stimulation effects can be achieved: in healthy or partially damaged brains residual structures are sufficient to allow electrical stimulation to influence ongoing oscillations and to enhance the power of the dominating band [14,18,31,62–64]. However, when the number of intact optic nerve fibers is below a critical minimum – as was the case in our severe optic nerve crush model – retinofugal activation is too low to produce sufficient physiological drive in higher cortical visual areas and can not entrain brain rhythms. However, as we showed here, current applied to the cornea is still able to modulate the visually deprived brain and reduce cortical idling. However, only when such current effect is fully understood can we take advantage of the full potential of non-invasive alternating current stimulation to improve sight of patients with vision loss.

References

[1] Bechtereva NP, Shandurina AN, Khilko VA, et al. Clinical and physiological basis for a new method underlying rehabilitation of the damaged visual nerve function by direct electric stimulation. Int J Psychophysiol 1985 Apr;2(4):257–72.

[2] Antal A, Kincses TZ, Nitsche MA, Bartfai O, Paulus W. Excitability changes induced in the human primary visual cortex by transcranial direct current stimulation:direct electrophysiological evidence. Invest Ophthalmol Vis Sci 2004;2:702–7.

[3] Antal A, Kincses TZ, Nitsche MA, Paulus W. Manipulation of phosphene thresholds by transcranial direct current stimulation in man. Exp Brain Res 2003;3:375–8.

[4] Antal A, Nitsche MA, Paulus W. Transcranial direct current stimulation and the visual cortex [Review] Brain Res Bull 2006;(6):459–63.

[5] Antal A, Paulus W, Nitsche MA. Electrical stimulation and visual network plasticity [Review] Restor Neurol Neurosci 2011;29(6):365–74.

[6] Fujikado T, Morimoto T, Matsushita K, Shimojo H, Okawa Y, Tano Y. Effect of transcorneal electrical stimulation in patients with nonarteritic ischemic optic neuropathy or traumatic optic neuropathy. Jpn J Ophthalmol 2006;3:266–73.

[7] Kanai R, Chaieb L, Antal A, Walsh V, Paulus W. Frequency-dependent electrical stimulation of the visual cortex. Curr Biol 2008;23:1839–43.

[8] Chaieb L, Antal A, Paulus W. Gender-specific modulation of short-term neuroplasticity in the visual cortex induced by transcranial direct current stimulation. Vis Neurosci 2008;1:77–81.

[9] Fedorov A, Chibisova Y, Szymaszek A, Alexandrov M, Gall C, Sabel BA. Non-invasive alternating current stimulation induces recovery from stroke. Restor Neurol Neurosci 2010;6:825–33.

[10] Fedorov A, Jobke S, Bersnev V, et al. Restoration of vision after optic nerve lesions with noninvasive transorbital alternating current stimulation:a clinical observational study. Brain Stimul 2011;4:189–201.

[11] Gall C, Antal A, Sabel BA. Non-invasive electrical brain stimulation induces vision restoration in patients with visual pathway damage. Graefes Arch Clin Exp Ophthalmol 2013;3:1041–3.

[12] Gall C, Fedorov AB, Ernst L, Borrmann A, Sabel BA. Repetitive transorbital alternating current stimulation in optic neuropathy. NeuroRehabilitation 2010;4:335–41.

[13] Gall C, Sgorzaly S, Schmidt S, Brandt S, Fedorov A, Sabel BA. Noninvasive transorbital alternating current stimulation improves subjective visual functioning and vision-related quality of life in optic neuropathy. Brain Stimul 2011;4:175–88.

[14] Sabel BA, Fedorov AB, Naue N, Borrmann A, Herrmann C, Gall C. Non-invasive alternating current stimulation improves vision in optic neuropathy. Restor Neurol Neurosci 2011;6:493–505.

[15] Sabel BA, Henrich-Noack P, Fedorov A, Gall C. Vision restoration after brain and retina damage: the "residual vision activation theory". Prog Brain Res 2011;192:199–262.

[16] Oono S, Kurimoto T, Kashimoto R, Tagami Y, Okamoto N, Mimura O. Transcorneal electrical stimulation improves visual function in eyes with branch retinal artery occlusion. Clin Ophthalmol 2011;5:397–402.

[17] Schmidt S, Mante A, Rönnefarth M, Fleischmann R, Gall C, Brandt SA. Progressive enhancement of alpha activity and visual function in patients with optic neuropathy: a two-week repeated session alternating current stimulation study. Brain Stimul 2013;1:87–93.

[18] Fedorov AB, Chibisova AM, Tchibissova JM. Impulse modulating therapeutic electrical stimulation (IMTES) increases visual field size in patients with optic nerve lesions. Int Congr Ser 2005;1282:525–9.

[19] Bola M, Gall C, Moewes C, Fedorov A, Hinrichs H, Sabel BA. Brain functional connectivity network breakdown and restoration in blindness. Neurology 2014;6:542–51.

[20] Sautter J, Sabel BA. Recovery of brightness discrimination in adult rats despite progressive loss of retrogradely labelled retinal ganglion cells after controlled optic nerve crush. Eur J Neurosci 1993;6:680–90.

[21] Sautter J, Schwartz M, Duvdevani R, Sabel BA. GM1 ganglioside treatment reduces visual deficits after graded crush of the rat optic nerve. Brain Res 1991;1:23–33.

[22] Sabel BA. Restoration of vision I: sneurobiological mechanisms of restoration and plasticity after brain damage – a review [Review] Restor Neurol Neurosci 1999;2-3:177–200.

[23] Sabel BA, Kasten E, Kreutz MR. Recovery of vision after partial visual system injury as a model of postlesion neuroplasticity. Adv Neurol 1997;73:251–76.

[24] Morimoto T, Fujikado T, Choi JS, et al. Transcorneal electrical stimulation promotes the survival of photoreceptors and preserves retinal function in royal college of surgeons rats. Invest Ophthalmol Vis Sci 2007;10:4725–32.

[25] Morimoto T, Miyoshi T, Matsuda S, Tano Y, Fujikado T, Fukuda Y. Transcorneal electrical stimulation rescues axotomized retinal ganglion cells by activating endogenous retinal IGF-1 system. Invest Ophthalmol Vis Sci 2005;6:2147–55.

[26] Morimoto T, Miyoshi T, Sawai H, Fujikado T. Optimal parameters of transcorneal electrical stimulation (TES) to be neuroprotective of axotomized RGCs in adult rats. Exp Eye Res 2010;2:285–91.

[27] Ni YQ, Gan DK, Xu HD, Xu GZ, Da CD. Neuroprotective effect of transcorneal electrical stimulation on light-induced photoreceptor degeneration. Exp Neurol 2009;2:439–52.

[28] Henrich-Noack P, Lazik S, Sergeeva E, et al. Transcorneal alternating current stimulation after severe axon damage in rats results in "long-term silent survivor" neurons. Brain Res Bull 2013;95:7–14.

[29] Henrich-Noack P, Voigt N, Prilloff S, Fedorov A, Sabel BA. Transcorneal electrical stimulation alters morphology and survival of retinal ganglion cells after optic nerve damage. Neurosci Lett 2013;543:1–6.

[30] Rousseau V, Engelmann R, Sabel BA. Restoration of vision III: soma swelling dynamics predicts neuronal death or survival after optic nerve crush in vivo. Neuroreport 1999;16:3387–91.

[31] Sergeeva EG, Fedorov AB, Henrich-Noack P, Sabel BA. Transcorneal alternating current stimulation induces EEG "aftereffects" only in rats with an intact visual system but not after severe optic nerve damage. J Neurophysiol 2012;9:2494–500.

[32] Nunez PL, Srinivasan R, Westdorp AF, et al. EEG coherency. I: statistics, reference electrode, volume conduction, Laplacians, cortical imaging, and interpretation at multiple scales. Electroencephalogr Clin Neurophysiol 1997;5:499–515.

[33] Pereda E, Quiroga RQ, Bhattacharya J. Nonlinear multivariate analysis of neurophysiological signals. Prog Neurobiol 2005;1-2:1–37.

[34] Prilloff S, Noblejas MI, Chedhomme V, Sabel BA. Two faces of calcium activation after optic nerve trauma:life or death of retinal ganglion cells in vivo depends on calcium dynamics. Eur J Neurosci 2007;11:3339–46.

[35] Wiesel TN, Hubel DH. Effects of visual deprivation on morphology and physiology of cells in the cats lateral geniculate body. J Neurophysiol 1963;26:978–93.

[36] Steriade M, Llinás RR. The functional states of the thalamus and the associated neuronal interplay [Review] Physiol Rev 1988;3:649–742.

[37] Kaplan AI, Novikova LA, Pevzner MS. Electrical activity of the brain in basic clinical forms of childhood blindness. Oftalmol Zh 1970;5:381–2.

[38] Zislina NN, Novikova LA. Effect of visual deafferentation on background and evoked activity of cerebral cortical neurons in the rabbit. Zh Vyssh Nerv Deiat Im I P Pavlova 1971;6:1298–306.

[39] Vuillon-Cacciuttolo G, Seri B. Effects of optic nerve section in baboons on the EEG activity and sleep-waking cycles. Electroencephalogr Clin Neurophysiol 1978;6:769–77.

[40] Eysel UT. Maintained activity, excitation and inhibition of lateral geniculate neurons after monocular deafferentation in the adult cat. Brain Res 1979;2:259–71.

[41] Ricardo JA, Negrão N, Pereira JS. ECoG effects of peripheral deafferentation of prepyriform and visual cortices in rats. Physiol Behav 1980;4:727–36.

[42] Eysel UT, Schweigart G, Mittmann T, et al. Reorganization in the visual cortex after retinal and cortical damage. Restor Neurol Neurosci 1999;2-3:153–64.

[43] Théoret H, Merabet L, Pascual-Leone A. Behavioral and neuroplastic changes in the blind:evidence for functionally relevant cross-modal interactions. J Physiol Paris 2004;1-3:221–33.

[44] Adrian ED, Matthews BH. The interpretation of potential waves in the cortex. J Physiol 1934;4:440–71.

[45] Mulholland T. Human EEG, behavioral stillness and biofeedback. Int J Psychophysiol 1995;3:263–79.

[46] Pfurtscheller G. Event-related synchronization (ERS): an electrophysiological correlate of cortical areas at rest. Electroencephalogr Clin Neurophysiol 1992;1:62–9.

[47] Pfurtscheller G, Neuper C. Event-related synchronization of mu rhythm in the EEG over the cortical hand area in man. Neurosci Lett 1994;1:93–6.

[48] Salmelin R, Hari R. Spatiotemporal characteristics of sensorimotor neuromagnetic rhythms related to thumb movement. Neuroscience 1994;2:537–50.

[49] Toro C, Deuschl G, Thatcher R, Sato S, Kufta C, Hallett M. Event-related desynchronization and movement-related cortical potentials on the ECoG and EEG. Electroencephalogr Clin Neurophysiol 1994;5:380–9.

[50] Pfurtscheller G, Stancák Jr A, Neuper C. Event-related synchronization (ERS) in the alpha band–an electrophysiological correlate of cortical idling:a review. Int J Psychophysiol 1996;1-2:39–46.

[51] Klimesch W. EEG alpha and theta oscillations reflect cognitive and memory performance:a review and analysis [Review] Brain Res Brain Res Rev 1999;2-3:169–95.

[52] Patino L, Chakarov V, Schulte-Mönting J, Hepp-Reymond MC, Kristeva R. Oscillatory cortical activity during a motor task in a deafferented patient. Neurosci Lett 2006;3:214–8.

[53] Kuhlman WN. Functional topography of the human mu rhythm. Electroencephalogr Clin Neurophysiol 1978;1:83–93.

[54] Suzuki H, Ichijo M. Tonic inhibition in the cat lateral geniculate nucleus maintained by retinal spontaneous discharge. Jpn J Physiol 1967;5:599–612.

[55] Nakai Y, Domino EF. Reticular facilitation of visually evoked responses by optic tract stimulation before and after enucleation. Exp Neurol 1968;4:532–44.

[56] Keck T, Scheuss V, Jacobsen RI, et al. Loss of sensory input causes rapid structural changes of inhibitory neurons in adult mouse visual cortex. Neuron 2011;5:869–82.

[57] Potts AM, Inoue J. The electrically evoked response (EER) of the visual system. II. Effect of adaptation and retinitis pigmentosa. Invest Ophthalmol 1969;6:605–12.

[58] Potts AM, Inoue J. The electrically evoked response of the visual system (EER). 3. Further contribution to the origin of the EER. Invest Ophthalmol 1970;10:814–9.

[59] Potts AM, Inoue J, Buffum D. The electrically evoked response of the visual system (EER). Invest Ophthalmol 1968;3:269–78.

[60] Foik AT, Kublik E, Sergeeva EG, Tatlisumak T, Rossini PM, Sabel BA, Waleszczyk WJ. Retinal origin of electrically evoked potentials in response to transcorneal alternating current stimulation in the rat. Invest Ophthalmol Vis Sci 2015;3:1711–8.

[61] Sergeeva EG, Henrich-Noack P, Gorkin AG, Sabel BA. Preclinical model of transcorneal alternating current stimulation in freely moving rats. Restor Neurol Neurosci 2015 [Epub ahead of print].

[62] Zaehle T, Rach S, Herrmann CS. Transcranial alternating current stimulation enhances individual alpha activity in human EEG. PLoS One 2010;11:e13766.

[63] Herrmann CS, Rach S, Neuling T, Strüber D. Transcranial alternating current stimulation:a review of the underlying mechanisms and modulation of cognitive processes [Review] Front Hum Neurosci 2013;7:279.

[64] Neuling T, Rach S, Herrmann CS. Orchestrating neuronal networks:sustained after-effects of transcranial alternating current stimulation depend upon brain states. Front Hum Neurosci 2013;7:161.